Published in final edited form as:
Langmuir. 2013 November 19; 29(46): 14222–14229. doi:10.1021/la403124u.

Strong adhesion and cohesion of chitosan in aqueous solutions

Dong Woog Lee[a], **Chanoong Lim**[b], **Jacob N. Israelachvili**[a,c,*], and **Dong Soo Hwang**[b,d,e,f,*]

[a]Department of Chemical Engineering, University of California at Santa Barbara, CA 93106, USA

[b]School of Interdisciplinary Bioscience and Bioengineering, Pohang University of Science and Technology (POSTECH), Pohang 790-784, South Korea

[c]Materials Department, University of California at Santa Barbara, CA 93106, USA

[d]School of Environmental Science and Engineering, Pohang University of Science and Technology (POSTECH), Pohang 790-784, South Korea

[e]POSTECH Ocean Science and technology Institute (POSTI), Pohang University of Science and Technology (POSTECH), Pohang 790-784, South Korea

[f]Integrative Biosciences and Biotechnology, Pohang University of Science and Technology (POSTECH), Pohang 790-784, South Korea

Abstract

Chitosan, a load-bearing biomacromolecule found in the exoskeletons of crustaceans and insects, is a promising biopolymer for the replacement of synthetic plastic compounds. Here, surface interactions mediated by chitosan in aqueous solutions, including the effects of pH and contact time, were investigated using a surface forces apparatus (SFA). Chitosan films showed an adhesion to mica for all tested pH ranges (3.0–8.5), achieving a maximum value at pH 3.0 after a contact time of 1 hr (W_{ad} ~6.4 mJ/m^2). We also found weak or no *cohesion* between two opposing chitosan layers on mica in aqueous buffer until the critical contact time for maximum *adhesion* (chitosan-mica) was reached. Strong cohesion (W_{co} ~8.5 mJ/m^2) between the films was measured with increasing contact times up to 1 hr at pH 3.0, which is equivalent to ~60% of the strongest, previously reported, mussel underwater adhesion. Such time-dependent adhesion properties are most likely related to molecular or molecular group reorientations and interdigitations. At high pH (8.5), the solubility of chitosan changes drastically, causing the chitosan-chitosan (cohesion) interaction to be repulsive at all separation distances and contact times. The strong contact time and pH-dependent chitosan-chitosan cohesion and adhesion properties provide new insight into the development of chitosan based load-bearing materials.

Keywords

chitosan; Surface forces apparatus; pH; interaction; contact time; cohesion

Introduction

Chitin, the major structural component in the exoskeletons of crustaceans and insects, is the second most abundant natural biopolymer after cellulose.[1-4] However, its application is

*To whom correspondence should be addressed. dshwang@postech.ac.kr, Phone: +82(54) 279-9505, Fax: +82(54) 279-9519. Jacob@engineering.ucsb.edu, Phone: (805) 893-8407, Fax: (805) 893-7870.

Supporting Information Available

Figure S1. Degree of deacetylation (DD) of chitosan molecule used in this study by 1H NMR Measurement is available free of charge via the Internet at http://pubs.acs.org/.

limited as chitin is a biopolymer that is not soluble in water or other common organic solvents. For this reason, chitin is generally converted to its partially deacetylated derivative, chitosan, which is soluble in dilute acidic medium.[2, 5] Chitin and chitosan compose a family of linear structural polysaccharides that consist of varying amounts of *N*-acetyl-D-glucosamine and D-glucosamine units connected by β-1,4 linkages (Figure 1). The degree of acetylation (DA) which represents a percentage of *N*-acetyl-D-glucosamine unit with respect to the total number of the two units defines the two terms, chitin and chitosan, and affects their solubility in dilute acidic medium ($2 < pH < 6$). Conventionally, the DA value of chitosan is usually considered to be below 50%, while chitosan is soluble in dilute acidic buffer. However, a specific DA to characterize chitin versus chitosan has not yet been determined.[6]

Chitosan is one of the most widely used biopolymers for numerous applications in various fields such as fabrics,[3] cosmetics,[7] water treatment,[8] and food processing[9] due to its ability to bind to a variety of natural or synthetic molecules such as nanoparticles, drugs, polymers, metal ions, and cells. Accordingly, formulations of chitosan with such molecules have been prepared in a wide range of forms including films, hydrogels, fibers and emulsions and have been utilized in numerous fields.[9] Moreover, chitosan is also a highly attractive biomaterial in the medical and pharmaceutical fields because of its low toxicity and biodegradability as well as wound healing and antimicrobial activity.[10]

In spite of these many applications of chitosan, there have been few systematic studies conducted with regards to the interaction between chitosan with other substrates and itself. Chitosan can form fibrous self-assembled structures based on hydrogen bond networks in aqueous solutions, and conformational variations of the chitosan assembly has been reported[11] to depend on local environment changes around chitosan (e.g., pH, temperature, types of salt, and types of acids).[12-18] Therefore, understanding the interactions of chitosan under different aqueous buffer conditions is useful for the interpretation and application of chitin/chitosan based biological materials. Only Claesson and Ninham measured pH-dependent interaction forcecs between adsorbed chitosan layers by a surface forces apparatus (SFA),[19] an instrument that has been widely used to measure the intermolecular forces in various biological systems[20-23] with nano-Newton force sensitivity and angstrom distance resolution.[24] These authors measured rather small adhesion forces of chitosan to mica or chitosan itself (W_{co} ~0.5 mJ/m^2). This behavior is not inconsistent with semicrystalline phase formation of chitosan fibers depending on the degree of deacetylations. In addition, chitosan has reactive primary amine groups with a hydrophilic helical structure, which help to form various intermolecular and intramolecular interactions. Therefore, we hypothesize that longer contact times during the force measurement compared to the previous study might enhance cohesion/adhesion between two opposing chitosan layers or between a chitosan layer and mica.

Here, unlike in the previous SFA study, the effects of contact time on chitosan interactions in aqueous solutions were investigated using a SFA, because longer contact times can induce molecular reorientations and interdigitations that can significantly increase adhesion and/or cohesion.[25] Our results suggest that the contact time plays a critical role in the strong cohesion between chitosan films, which is likely due to molecular reorientations and interdigitations of the chitosan film during prolonged contact times.

Materials and Methods

Materials

Chitosan (MW 120,000–150,000) was purchased from Sigma-Aldrich. The solubility of chitosan was ~ 80 mg/mL in 150 mM acetic acid at 25°C and the chitosan was only soluble

in acetate buffer solutions of pH below 6.5 The degree of acetylation (DA) of chitosan was determined by ^{1}H NMR.[26] For the ^{1}H NMR measurement, chitosan was suspended in DCl and were acquired with 16 transients, acquisition time of 3.642 sec and a delay of 1.500 sec. The temperature was controlled at 70°C to increase chitosan solubility. The degree of acetylation of chitosan was calculated from the areas of the signals in 2.1 ppm (methyl) and sum of the areas from 3.2 to 4.2 ppm (H2, H3, H4, H5, H6, and H6) in the ^{1}H NMR according to formula (1).

$$\%DA = \left(\frac{2A_{\mathrm{CH_3}}}{A_{\mathrm{H2H6}}}\right) \times 100 \quad (1)$$

To prepare chitosan solutions (10 μg/ml), chitosan was dissolved in a 150 mM acetic acid (pH 3.0) solution. Three buffers with different pHs were prepared: 150 mM acetic acid (pH 3.0), 150 mM sodium acetate buffer (pH 6.5), and 150 mM phosphate buffer (pH 8.5).

Preparation of surface

Atomically smooth mica surfaces (Grade #1, S&J Trading, Inc.) were freshly cleaved under a laminar flow hood and placed on another large freshly cleaved mica backing sheet. A silver layer (Cerac, purity > 99.99%) of uniform thickness (55 nm) was deposited using a Joule effect vapor deposition. Before chitosan deposition, the silvered mica sheets were glued (silver side down) on cylindrical glass disks using an epoxy glue (EPON 1004 F®, Exxon Chemicals).[27, 28]

Interaction forces measurement using a Surface Forces Apparatus (SFA)

The normal force-distance profiles and cohesion/adhesion forces of chitosan films were determined using a surface forces apparatus 2000 in a configuration that was previously reported in literature.[24, 29] Chitosan was physically deposited on the back silvered mica. The glued mica surface was dipped into a prepared chitosan solution (10 μg/ml in 150 mM acetic acid, pH 3.0) for 20 min followed by a thorough rinsing with the buffer solution (150 mM acetic acid, pH 3.0) in order to remove unbound chitosan. Depending on the experiment conducted, either two chitosan coated surfaces (symmetric) or one chitosan coated surface and one bare mica surface (asymmetric) were transferred into the SFA chamber in crossed-cylinder geometry which corresponds to a sphere of radius R approaching a flat surface based on the Derjaguin approximation.[30] A droplet (50 μl) of buffer (pH 3.0) was injected between the transferred surfaces. The SFA chamber was sealed and saturated with water vapor during the experiments. After mounting of the surfaces and injection of the buffer, the system was allowed to equilibrate for 1 hr. All experiments were conducted at room temperature (T=23°C). The force (F) was measured by determining the deflection of the double cantilever spring (k = 3030 N/m) of the lower surface, and the distance (D) between two mica surfaces was measured from the “fringes of equal chromatic order (FECO)” using optical interferometry.[27] The lower surface was connected to a motor, which allows the two surfaces to move relative to each other at a controlled speed (~3 nm/s in this study). R is the radius of the cylindrical silica disk (usually ~2 cm) and D is the surface separation distance between two bare mica surfaces. The measured adhesion or normalized “pull-off” force F_{ad}/R (= − min[F/R]) is related to the adhesion energy per unit area W_{ad} by $W_{ad} = 2F_{ad}/3\pi R$, the Johnson-Kendall-Roberts (JKR) model for soft materials with large deformations,[28, 30] while for calculating the surface energy during approach, which was always repulsive without flattening of the surfaces, the Derjaguin approximation, $W = F/2\pi R$, was used.[28, 30] The surfaces were approached to contact (around F/R~4 mN/m) and kept in contact for durations of 5 sec, 2 min, 10 min, and 1 hr, followed by separation to investigate the effect of contact time on cohesion/adhesion forces of the chitosan films. Force *vs* distance profiles

were measured multiple times at each condition to confirm their reproducibility. In addition to the force measurement under the pH 3.0 buffer, the measurements were repeated after replacing the buffer with an excess amount of 150 mM sodium acetate buffer solution (pH 6.5) and 150 mM phosphate buffer solution (pH 8.5) to study the effects of pH.

Atomic force microscopy (AFM)

Freshly cleaved mica surfaces were dipped into a prepared chitosan solution (10 μg/ml in 150 mM acetic acid, pH 3.0) for 20 min followed by a thorough rinsing with the buffer solution (150 mM acetic acid, pH 3.0) in order to remove unbound chitosan. The chitosan film on mica surface was incubated for 1hr under three different pHs (3.0, 6.5, 8.5). Images were acquired using a Nanoscope III AFM (Veeco, Santa Barbara, CA, USA) using a silicon nitride probe (Olympus, Tokyo, Japan), with a spring constant of 0.35 N m^{-1}. Scanning was performed in tapping mode at room temperature (22±1°C)

Results and discussion

Chitosan adsorption on mica

Adhesion and cohesion of chitosan can be influenced by the degree of deacetylation (DDA) of chitosan which modifies its crystalline structure. Therefore, the degree of acetylation (DA) of chitosan was estimated by ^{1}H NMR measurement prior to the SFA experiment. The DA of chitosan used in this study was ~19 % (See Figure S1). The interaction forces between two layers of chitosan adsorbed on mica surfaces or between chitosan film and mica were measured using an SFA. The adsorption of chitosan to mica was mainly driven by electrostatic attraction between positively charged chitosan molecules at pH 3.0 and negatively charged mica surfaces. The surfaces were thoroughly washed with 0.15 M acetic acid to remove unbound chitosan molecules before the SFA experiment. The adsorption of chitosan to mica was confirmed by the increase in the steric wall distance (D_{sw}; defined as the D at F/R~4 mN/m). The thickness of chitosan films, as measured by D_{sw}, was ~1.5 nm per surface, which is similar to values reported by a previous study.[19] Although a comprehensive configuration of chitosan film on mica is difficult to resolve experimentally, D_{sw} from the SFA experiments can give some clues to deduce the configuration of chitosan film on mica. The measured contour length of chitosan used in this study was around 1000 nm [31] and the radius of gyration of chitosan (R_g) expected by the empirical equation,[32] $R_g=0.075\cdot(MW)^{0.55}$, is ~50 nm in an acidic environment. The R_g of chitosan with a similar molecular weight in acidic buffer determined by dynamic light scattering was also ~50 nm.[33]

The repulsive force started around D > 20 nm on approach (Fig. 2A) with a decay length of ~7 nm, indicating that a swollen structure (exposing loops) of initially adsorbed chitosan. And the measured decay length on approach might be related to the thickness of loops of initial chitosan structure. After the compression (up to F/R~4 mN/m) the film thickness as measured by D_{sw} of one chitosan film (~1.5 nm) at pH 3.0 was much less than the expected radius of gyration of 50 nm.[32, 33] Consequently, these measurements indicate that chitosan would be in a flat conformation under cofinement.[34] Also, there was no observed hysteresis on approach, possibly due to rapid changes to the initial swollen structure on separation by pulling out the looped residues of chitosan molecules from adhesive contact.

Cohesion of chitosan films (symmetric configuration)

Contact time effect—At pH 3.0, normalized cohesion forces between the two chitosan films, F_{co}/R (= −min[F/R]), on the separation depended mostly on the contact time, t_{ct} (Figure 2A). No cohesion was initially measured between two chitosan films at t_{ct} ~5 sec and the surfaces were purely repulsive with steric wall, D_{sw}, of ~3 nm. However, as t_{ct}

increases from 2 min to 1 hr, the following results were observed: i) the repulsion disappeared and F_{co}/R increased from ~2 to ~40 mN/m and the right hand y-axis shows that these forces correspond to surface cohesion energies of W_{co} from ~0.4 to ~8.5 mJ/m^2. ii) D_{sw} decreased from ~3 nm to ~1 nm. iii) Repeated contact and separation with 5 sec of t_{ct} after breaking the 1 hr contact produced a W_{co} of ~0.85 mJ/m^2. Previous studies with chitosan films only showed a relatively weak cohesion force of ~0.5 mN/m (W_{co} ~0.1 mJ/m^2) at pH 3.8 with 2 mM of acetic acid, which is probably due to relatively short contact time.[19] The cohesive energy W_{co} of ~8.5 mJ/m^2 measured in the present study is about 60% of the interaction between the strongest, previously reported, mussel adhesive protein to mica (Mefp-5 to mica, W_{ad} ~14 mJ/m^2).[35]

Effects of pH on cohesion of chitosan—Figure 2 shows the interaction forces between two chitosan physisorbed surfaces (symmetric configuration, see the schematic in Fig. 2A) in 0.15 M buffer solutions at three pHs (3.0, 6.5 and 8.5). As the previously reported pKa value of chitosan is around 6.5–7.0, we chose pH 3.0 as most glucosamine units in chitosan would be protonated, pH 6.5 as where half of the glucosamine would be protonated, and pH 8.5 where the most glucosamine would be not protonated. The cohesion energy, W_{co}, of chitosan films decreased with increasing pH, from ~8.5 mJ/m^2 at pH 3.0 to ~1.7 mJ/m^2 at pH 6.5, and 0 mJ/m^2 at pH 8.5. On the other hand, D_{sw} increased with increasing pH, from ~2.5 nm at pH 3.0, ~3 nm at pH 6.5, and ~24 nm at pH 8.5. These results are consistent with the previous work done by Claesson and Ninham[19] which also showed a decrease in adhesion force and increase in the chitosan layer thickness with increase in pH. To confirm that the chitosan thickness increased while increasing the buffer pH, we prepared equivalent adsorbed chitosan surfaces on mica. The root mean square (RMS) surface roughness determined by Atomic force microscopy (AFM) for surfaces at pH 3.0, 6.5 and 8.5 were 0.14 nm, 0.30 nm and 0.96 nm, respectively (See Fig. 3). AFM topology of the chitosan film on mica showed that chitosan layers were roughened by increasing the solution pH, as observed in the SFA. Since the adhesion between two elastic surfaces is generally reduced with increasing the surface roughness,[36] the lack of adhesion between two opposing chitosan surfaces at pH 8.5 was also influenced by the surface roughness.

Proposed mechanism for cohesion of two opposed chitosan layers—It was previously demonstrated using the SFA that the thickness of adsorbed chitosan on mica was not increased even after 24 hrs of incubation with 0.01 % (w/v) acetic acid containing 0.01 % (w/v) chitosan. This suggested that chitosan molecules initially might not have cohesion in acetic acid solutions.[19] Consistent with the previous study, two opposed positively charged chitosan films did not have any cohesive interaction in acetate buffers with a short contact time. However, with an increase in the contact time, cohesion between the chitosan layers began to occur. Additionally, higher contact times resulted in higher cohesive energy and lower D_{sw} between two opposing chitosan films. These observations are typical signs of molecular rearrangement and cohesive bond* sformation while the surfaces are in contact. The increase in cohesion with time was probably due to a rearrangement of chitosan molecules into an orientation proper for cohesion while in contact with the opposing surface, resulting in stronger cohesive interaction over time. Indeed, conformational transitions of chitosan molecules have been reported to occur as the local environment around the chitosan molecule changes (pH, temperature, and types of acid and salts).[15] Up to now, four types of X-ray crystal structures of chitosan (Extended two-fold helix, Relaxed two-fold helix, 4/1 helix, and 5/3 helix) have been identified, each depending on the local environment. Since

*Cohesive/adhesive bond indicated in this study include physical bonds induced by all types of attractive interactions such as electrostatic, hydrophobic, and van der Waals'.

4/1 helix and 5/3 helix only occur in the presence of iodide ions and aromatic organic acids, respectively, these helixes are not likely to be formed in the present study.[12, 13] It is reported that chitosan prefers to take up a relaxed two-fold helix structure which doesn't form strong intramolecular hydrogen bonds in acetate buffer systems[16, 18] similar to what we used in our SFA experiments. Therefore, chitosan molecules adsorbed on mica would initially exhibit a relaxed two-fold helix with higher thickness (See summary and conclusion). Based on the D_{sw} reduction with the increase of t_{ct} (from 3 nm to 1 nm), chitosan molecules adsorbed to mica presumably changed to an extended two-fold helix, which is a zigzag structure similar to those of chitin and cellulose.[16, 18] The contact time effects imply that strong cohesion may arise from a conformational change from a relaxed two-fold helix to an extended two-fold helix, caused by confinement of chitosan chains at the contact. Consequently, the structural change is enhanced at pH 3.0 due to the flexibility of the chitosan chains[37-39] that promotes its rearrangement to form hydrogen bonds and hydrophobic interactions against chitosan at the opposing surface (see Fig. 1 for hydrogen bonding sites). Furthermore, based on the DA measurement, chitosan used in this study was composed of 19 mol % of *N*-acetyl-D-glucosamine and 81 mol % of D-glucosamine. Relatively hydrophobic methyl groups in the *N*-acetyl-D-glucosamine unit would be initially hidden due to long incubation with aqueous buffer, but it could be exposed to the methyl group of *N*-acetyl-D-glucosamine on the other surface, resulting in increases in adhesion due to hydrophobic interactions. Both hydrogen bonds and hydrophobic interactions of the methyl groups are likely to be responsible for the exceptionally high cohesion force between the chitosan physisorbed surfaces. Successive force measurements (t_{ct} = 5 sec) right after the force run with t_{ct} of 1 hr were quite reproducible, implying that proper orientation for strong cohesion can be maintained for a certain amount of time.

Besides the rearrangement and structural change of chitosan chains, ion diffusion/migration and charge regulation established at the contact could be a factor in decreasing electrostatic repulsion which, in turn, increases the adhesion force. The charge regulation can affect the interaction forces between chitosan surfaces, but the adhesion forces due to hydrogen bonding and hydrophobic attraction are dominant. Also, in this system with a high anion concentration (15 - 150 mM), charge regulation will occur in a very short time; thus, chitosan rearrangement will likely to be the rate-limiting step.

At pH 6.5, amine groups in chitosan are less protonated compared to pH 3.0, causing the chitosan chains to be less flexible.[40] Accordingly, D_{sw} is thicker and F_{co} is significantly smaller (~1.6 mJ/m^2 at t_{ct} = 1 hr) compared to pH 3.0 (See Fig. 2B). In other words, it takes more time for chitosan chains to change their conformation. At pH 8.5, most of the amine groups are not protonated and the solubility of chitosan decreases drastically, making chitosan layers extremely rigid and immobile. As a result, D_{sw} significantly thickens (~23 nm) and the force profiles between chitosan physisorbed surfaces become purely repulsive due to steric repulsion (see Fig. 2C) which overwhelms all other attractive interaction forces. Also, at this pH, chitosan chains are too rigid to rearrange and form hydrogen bonds or exhibit noticeable hydrophobic attraction in a short time (t_{ct} < 1 hr).

Chitosan adhesion to mica (asymmetric configuration)

Effect of contact time and pH—Figure 4 shows the interaction forces between chitosan physisorbed surfaces and mica (see the schematic in Fig. 4A). The same experimental conditions (pH and t_{ct}) are applied as the symmetric case (Fig. 2) in order to see the normalized adhesion force, F_{ad}/R (= − min[F/R]), of chitosan layer to mica. In contrast to the symmetric configuration, a strong adhesion F_{ad}/R ~18 mN/m (W_{ad} ~3.8 mJ/m^2) was observed at pH 3.0 with only a 5 second contact. The thickness of one chitosan layer measured by D_{sw} was similar to the symmetric configuration (~1.5 nm). When the chitosan

film stayed in contact with mica, W_{ad} reached a plateau at the 10 min contact time (Figure 4A). The adhesion significantly decreased with increasing buffer pH from W_{ad} ~3.8 mJ/m^2 at pH 3.0 to W_{ad} ~0.6 mJ/m^2 at pH 6.5, and W_{ad} ~0.4 mJ/m^2 at pH 8.5 (Figure 4B and 4C). On the other hand, W_{ad} did not plateau at higher pH unlike pH 3.0, and was still increasing with increasing contact time (Figure 5B). The decrease of the adhesion of chitosan film to mica with increasing pH is likely to be related to the reduction of the positively charged D-glucosamine unit in chitosan, since it has a pKa of 6.5–7.0. Similar to symmetric cases, D_{sw} decreased with increase in contact time and increased with an increase in pH. The results show that the D_{sw} decrease and the F_{ad}/R increase with the increase in t_{ct} are similar to symmetric cases. However, the following discrepancies are observed compared to symmetric cases: i) repulsion is smaller on approach, ii) D_{sw} is smaller (up to ~50 %), iii) at pH 8.5, surfaces are adhesive, and iv) at pH 3.0, repeated contact and separation with 5 sec of t_{ct} after breaking the 1 hr contact produced an W_{ad} ~5.1 mJ/m^2, which is a rather small increase from ~3.8 mJ/m^2. These differences are expected, because the chitosan is only physisorbed to one surface and opposing surfaces are now under electrostatic attraction at pH 3.0 and 6.5 (negative mica and positive chitosan film). Meanwhile, at pH 8.5, even though most of the amines in chitosan are not protonated and electrostatic attraction is eliminated, the surfaces remain adhesive. This is due to the rapid formation of hydrogen bonds and van der Waals forces between mica and chitosan.

Contact time effects on the cohesion/adhesion forces

The rate of cohesive/adhesive bond formation depends both on the time needed to overcome electrostatic/steric repulsion (activation energy) and the mobility of chitosan chains for hydrogen donors to find hydrogen acceptors at opposing surfaces. These repulsions induce a critical time,[41, 42] t_{crit}, before chitosan changes structure and starts forming hydrogen bonds. t_{crit} highly depends on pH because increasing pH not only makes the chitosan chains neutral, but also decreases the solubility and makes the chains rigid and immobile.

Figure 5 shows the time evolution of the cohesion and adhesion forces which reveals important clues to understanding the system. In the case of the symmetric surfaces (Fig. 5A) at pH 3.0 and 6.5, the chitosan chains are fully and half protonated, respectively, and cause the surfaces to repel on approach. Moreover, the measured decay lengths are larger than the Debye lengths (see Fig. 6) indicating that steric repulsions between opposing chitosan chains are also significant. At pH 8.5, electrostatic repulsion is eliminated due to the deprotonation of the chitosan chains, but the higher rigidity induces even higher repulsion. The increase of t_{crit} with pH also indicates that the chitosan chains become more rigid and less mobile. For the symmetric case (Fig. 5A), t_{crit} was ~120 sec at pH 3.0, ~220 sec at pH 6.5, and at pH 8.5 it was too high to be measured (t_{crit} > 1 hr).

Meanwhile at pH 3.0 and 6.5, chitosan and mica surfaces (Fig. 5B) are electrostatically ‘attractive’. As a result, for pH 3.0 and 6.5, t_{crit} was too small to be measured (< 5 sec) and for pH 8.5, t_{crit} was ~100 sec. These results indicate that the time for chitosan to form an adhesive bond with mica was much faster than the chitosan surface forming cohesive bonds. For both the symmetric and asymmetric cases, when $t_{ct} > t_{crit}$, F_{co} and F_{ad} scaled as ~$t_{ct}^{1/2}$, which suggests that they are diffusion controlled processes, as previously reported.[43, 44] In this regime, chitosan molecules are adjusting their position and orientation by diffusion to form a conformation which can maximize the adhesion energy. As t_{ct} increases further, the adhesion and cohesion forces plateau to certain values as the rate of adhesive bond formation approaches zero.[41] This saturation was observed at pH 3.0 for the asymmetric case at t_{ct} ~400 sec. However, for the symmetric case, no complete saturation was observed even for 1 hr of contact time, indicating that the saturation occurs at t_{ct} > 1 hr.

Summary and Conclusion

The proposed chitosan interaction mechanisms are shown schematically in Figure 7. Based on the SFA results and discussions above, the interaction mechanisms between two opposed chitosan films (symmetric configuration) and between a chitosan film and mica (asymmetric configuration) can be summarized as follows:

1. For the symmetric configuration (chitosan *vs* chitosan cohesion), the critical contact time to achieve cohesion between two chitosan films was relatively long and the cohesive energy between the chitosan films at pH 3.0 was strong (W_{ad}~8.5 mJ/m^2), reaching nearly 60% of the strongest mussel adhesive protein (mefp-5) to mica. Here, we speculate that the contact time dependence of the self interactions of chitosan molecules is probably related to the formation of hydrogen bonds enhanced by structural changes in the chitosan molecules from a relaxed two-fold helix (a chitosan structure in dilute acetic acid) to an extended two-fold helix (a chitosan structure with zigzag structure which is similar to those of chitin and cellulose) due to the confinement of the chitosan films during contact.
2. For the asymmetric configuration (chitosan *vs* mica adhesion), chitosan strongly interacted with a negatively charged mica surface via electrostatic forces when the chitosan molecule is positively charged. However, it can also interact with the mica via other interaction forces such as hydrogen bonds and van der Waals forces between the D-glucosamine units in chitosan and hydrated mica surfaces.

In conclusion, we directly measured the strong molecular interactions of chitosan using an SFA; these measurements provided insights into the self-assembly of chitosan molecules in wet conditions. Our SFA study showed strong adhesive interactions between chitosan and mica, and strong cohesive strength between two opposed chitosan films in acidic buffer. The chitosan interactions decreased with increasing buffer pH, which is proposed to be mainly due to the reduction in solubility of chitosan molecules as they are not protonated at higher pH. Our results should be applicable to the use of chitosan in various biomedical applications.

Supplementary Material

Refer to Web version on PubMed Central for supplementary material.

Acknowledgments

D.S.H. and C. L. acknowledges the National Research Foundation of Korea Grant funded by the Korean Government (MEST) (NRF- C1ABA001- 2011-0029960). This work was supported by the MRSEC Program of the National Science Foundation under Award No. DMR 1121053. This research was also supported by the National Institutes of Health under award number R01 DE 018468. Authors thank Dr. J. Herbert Waite for fruitful discussion.

References

1. Guhha, RA.; Soares, TA.; Rusu, VH.; Pontes, FJS.; Franca, EF.; Lins, RD. The Molecular Structure and Conformational Dynamics of Chitosan Polymers: An Integrated Perspective from Experiments and Computational Simulations. Intech; Croatia: 2012.
2. Ifuku S, Nogi M, Abe K, Yoshioka M, Morimoto M, Saimoto H, Yano H. Preparation of Chitin Nanofibers with a Uniform Width as alpha-Chitin from Crab Shells. Biomacromolecules. 2009; 10(6):1584–1588. [PubMed: 19397258]
3. Kurita K. Chitin and chitosan: Functional biopolymers from marine crustaceans. Marine Biotechnology. 2006; 8(3):203–226. [PubMed: 16532368]

4. Kumar M. A review of chitin and chitosan applications. Reactive & Functional Polymers. 2000; 46(1):1–27.
5. Chang KLB, Tsai G, Lee J, Fu WR. Heterogeneous N-deacetylation of chitin in alkaline solution. Carbohydrate Research. 1997; 303(3):327–332.
6. Wang WP, Du YM, Qiu YL, Wang XY, Hu Y, Yang JH, Cai J, Kennedy JF. A new green technology for direct production of low molecular weight chitosan. Carbohydrate Polymers. 2008; 74(1):127–132.
7. Wei ZJ, Wang CY, Zou SW, Liu H, Tong Z. Chitosan nanoparticles as particular emulsifier for preparation of novel pH-responsive Pickering emulsions and PLGA microcapsules. Polymer. 2012; 53(6):1229–1235.
8. Riccardo AA, Uzzarelli M, Isolati A. Methyl mercury acetate removal from waters by chromatography on chelating polymers. Water Air and Soil Pollution. 1971; 1:65–71.
9. Yi HM, Wu LQ, Bentley WE, Ghodssi R, Rubloff GW, Culver JN, Payne GF. Biofabrication with chitosan. Biomacromolecules. 2005; 6(6):2881–2894. [PubMed: 16283704]
10. Kumar MNVR, Muzzarelli RAA, Muzzarelli C, Sashiwa H, Domb AJ. Chitosan chemistry and pharmaceutical perspectives. Chemical Reviews. 2004; 104(12):6017–6084. [PubMed: 15584695]
11. Ogawa K, Inukai S. X-Ray diffraction study of sulfuric, nitric, and halogen acid salts of chitosan. Carbohydrate Research. 1987; 160:425–433.
12. Kawahara M, Yui T, Oka K, Zugenmaier P, Suzuki S, Kitamura S, Okuyama K, Ogawa K. Fourth 3D structure of the chitosan molecule: Conformation of chitosan in its salts with medical organic acids having a phenyl group. Bioscience Biotechnology and Biochemistry. 2003; 67(7):1545–1550.
13. Lertworasirikul A, Tsue S, Noguchi K, Okuyama K, Ogawa K. Two different molecular conformations found in chitosan type II salts. Carbohydrate Research. 2003; 338(11):1229–1233. [PubMed: 12747866]
14. Ogawa K. Effect of Heating an Aqueous Suspension of Chitosan on the Crystallinity and Polymorphs. Agricultural and Biological Chemistry. 1991; 55:2375–2379.
15. Ogawa K, Yui T, Okuyama K. Three D structures of chitosan. International Journal of Biological Macromolecules. 2004; 34(1-2):1–8. [PubMed: 15178002]
16. Okuyama K, Noguchi K, Kanenari M, Egawa T, Osawa K, Ogawa K. Structural diversity of chitosan and its complexes. Carbohydrate Polymers. 2000; 41(3):237–247.
17. Okuyama K, Noguchi K, Miyazawa T, Yui T, Ogawa K. Molecular and crystal structure of hydrated chitosan. Macromolecules. 1997; 30(19):5849–5855.
18. Okuyama K, Osawa K, Hanafusa Y, Noguchi K, Ogawa K. Relaxed 2/1-helical conformation of type II chitosan has a tetrasaccharide motif. Journal of Carbohydrate Chemistry. 2000; 19(6):789–794.
19. Claesson PM, Ninham BW. PH-dependent interactions between adsorbed chitosan layers. Langmuir. 1992; 8(5):1406–1412.
20. Greene GW, Banquy X, Lee DW, Lowrey DD, Yu J, Israelachvili JN. Adaptive mechanically controlled lubrication mechanism found in articular joints. Proceedings of the National Academy of Sciences of the United States of America. 2011; 108(13):5255–5259. [PubMed: 21383143]
21. Lee DW, Banquy X, Israelachvili JN. Stick-slip friction and wear of articular joints. Proceedings of the National Academy of Sciences of the United States of America. 2013; 110(7):E567–E574. [PubMed: 23359687]
22. Lu QY, Danner E, Waite JH, Israelachvili JN, Zeng HB, Hwang DS. Adhesion of mussel foot proteins to different substrate surfaces. Journal of the Royal Society Interface. 2013; 10(79):11.
23. Sivasankar S, Brieher W, Lavrik N, Gumbiner B, Leckband D. Direct molecular force measurements of multiple adhesive interactions between cadherin ectodomains. Proceedings of the National Academy of Sciences of the United States of America. 1999; 96(21):11820–11824. [PubMed: 10518534]
24. Israelachvili J, Min Y, Akbulut M, Alig A, Carver G, Greene W, Kristiansen K, Meyer E, Pesika N, Rosenberg K, Zeng H. Recent advances in the surface forces apparatus (SFA) technique. Reports on Progress in Physics. 2010; 73(3):16.

25. Hwang DS, Zeng HB, Lu QY, Israelachvili J, Waite JH. Adhesion mechanism in a DOPA-deficient foot protein from green mussels. Soft Matter. 2012; 8(20):5640–5648. [PubMed: 23105946]
26. Hirai A, Odani H, Nakajima A. Determination of degree of deacetylation of chitosan by 1H NMR spectroscopy. Polymer Bulletin. 1991; 26:87–94.
27. Israelachvili J. Thin-film studies using multiple-beam interferometry. Journal of Colloid and Interface Science. 1973; 44(2):259–272.
28. Israelachvili, JN. Intermolecular and surface forces. 3. Academic Press and Elsevier; Amsterdam: 2011.
29. Hwang DS, Zeng HB, Masic A, Harrington MJ, Israelachvili JN, Waite JH. Protein- and Metal-dependent Interactions of a Prominent Protein in Mussel Adhesive Plaques. Journal of Biological Chemistry. 2010; 285(33):25850–25858. [PubMed: 20566644]
30. Johnson KL, Kendall K, Roberts AD. Surface energy and contact of elastic solids. Proceedings of the Royal Society of London Series a-Mathematical and Physical Sciences. 1971; 324(1558):301.
31. Hu Y, Wu YZ, Cai JY, Ma YF, Wang B, Xia K, He XQ. Self-assembly and fractal feature of chitosan and its conjugate with metal ions: Cu(II)/Ag(I). International Journal of Molecular Sciences. 2007; 8(1):1–12.
32. Rinaudo M. Chitin and chitosan: Properties and applications. Progress in Polymer Science. 2006; 31(7):603–632.
33. Wu C, Zhou SQ, Wang W. A dynamic laser light-scattering study of chitosan in aqueous-solution. Biopolymers. 1995; 35(4):385–392.
34. Lescanec RL, Muthukumar M. Configurational characteristics and scaling behavior of starburst molecules: a computational study. 1990; 23:2280–2288.
35. Danner EW, Kan YJ, Hammer MU, Israelachvili JN, Waite JH. Adhesion of Mussel Foot Protein Mefp-5 to Mica: An Underwater Superglue. Biochemistry. 2012; 51(33):6511–6518. [PubMed: 22873939]
36. Fuller KNG, Tabor D. Effect of surface-roughness on adhesion of elastic solids. Proceedings of the Royal Society of London Series a-Mathematical Physical and Engineering Sciences. 1975; 345(1642):327–342.
37. Franca EF, Freitas LCG, Lins RD. Chitosan Molecular Structure as a Function of N-Acetylation. Biopolymers. 2011; 95(7):448–460. [PubMed: 21328576]
38. Franca EF, Lins RD, Freitas LCG, Straatsma TP. Characterization of Chitin and Chitosan Molecular Structure in Aqueous Solution. Journal of Chemical Theory and Computation. 2008; 4(12):2141–2149.
39. Skovstrup S, Hansen SG, Skrydstrup T, Schiott B. Conformational Flexibility of Chitosan: A Molecular Modeling Study. Biomacromolecules. 2010; 11(11):3196–3207.
40. Chen RH, Tsaih ML, Lin WC. Effects of chain flexibility of chitosan molecules on the preparation, physical, and release characteristics of the prepared capsule. Carbohydrate Polymers. 1996; 31(3): 141–148.
41. Xu LC, Siedlecki CA. Effects of surface wettability and contact time on protein adhesion to biomaterial surfaces. Biomaterials. 2007; 28(22):3273–3283. [PubMed: 17466368]
42. Xu LC, Vadillo-Rodriguez V, Logan BE. Residence time, loading force, pH, and ionic strength affect adhesion forces between colloids and biopolymer-coated surfaces. Langmuir. 2005; 21(16): 7491–7500. [PubMed: 16042484]
43. Banquy X, Kristiansen K, Lee DW, Israelachvili JN. Adhesion and hemifusion of cytoplasmic myelin lipid membranes are highly dependent on the lipid composition. Biochimica Et Biophysica Acta-Biomembranes. 2012; 1818(3):402–410.
44. Meyer EE, Rosenberg KJ, Israelachvili J. Recent progress in understanding hydrophobic interactions. Proceedings of the National Academy of Sciences of the United States of America. 2006; 103(43):15739–15746. [PubMed: 17023540]

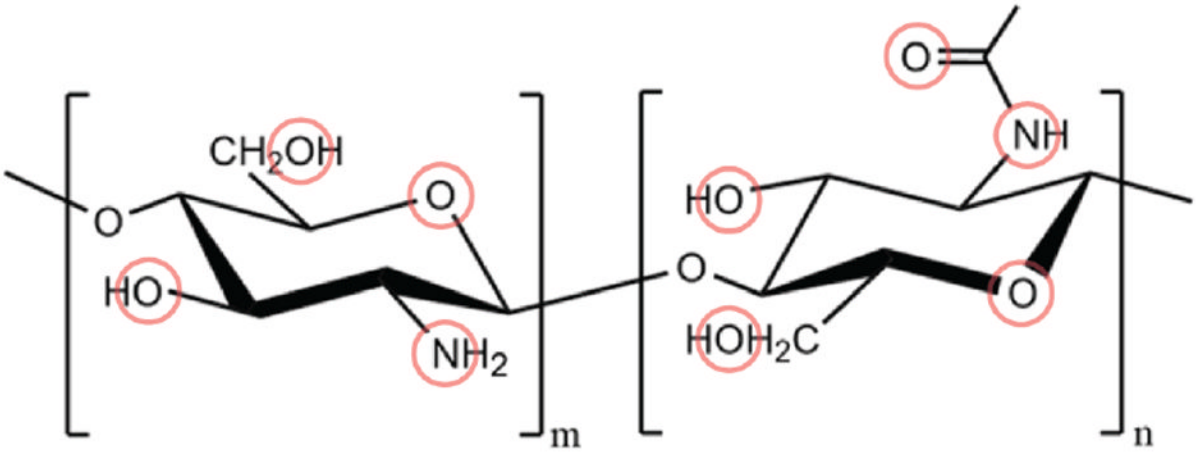

Figure 1.

Chemical structures of chitin and chitosan. Chitin and Chitosan are random copolymers of D-glucosamine (m) and *N*-acetyl-D-glucosamine (n) unit. (Chitin n>m;Chitosan m>n). Red circles indicate the hydrogen bonding sites.

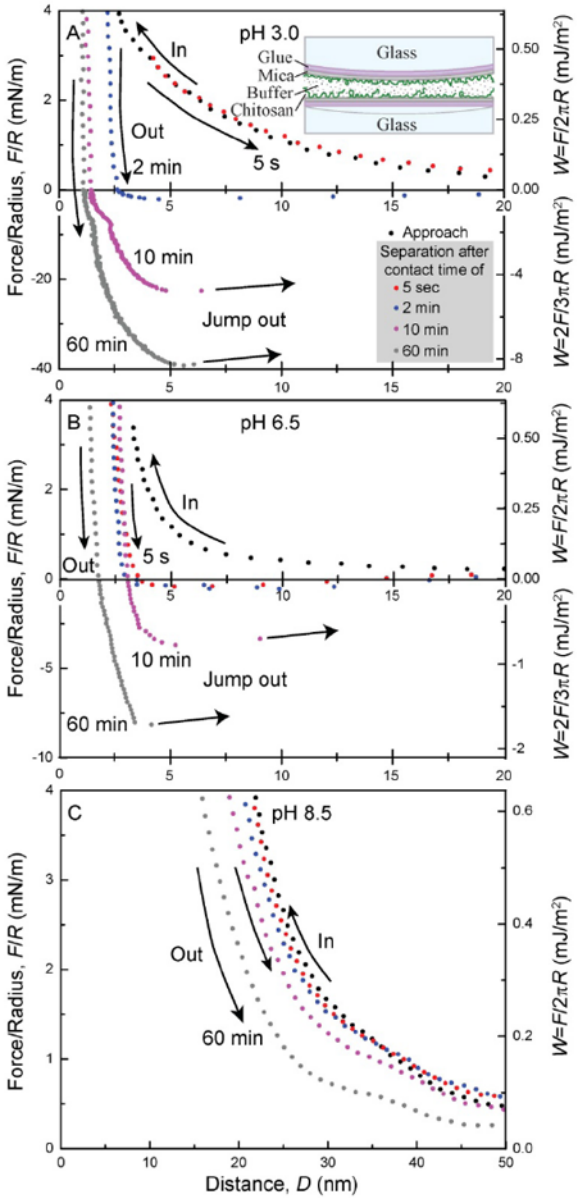

Figure 2.

Force profiles between two physisorbed chitosan surfaces in (A) pH 3.0 and 150 mM acetic acid solution, (B) pH 6.5 and 150 mM sodium acetate buffer solution, and (C) pH 8.5 and 150 mM phosphate buffer solution with the contact times of 5 sec, 2 min, 10 min, and 1 hr. All force curves are the representative results at each experiment conditions.

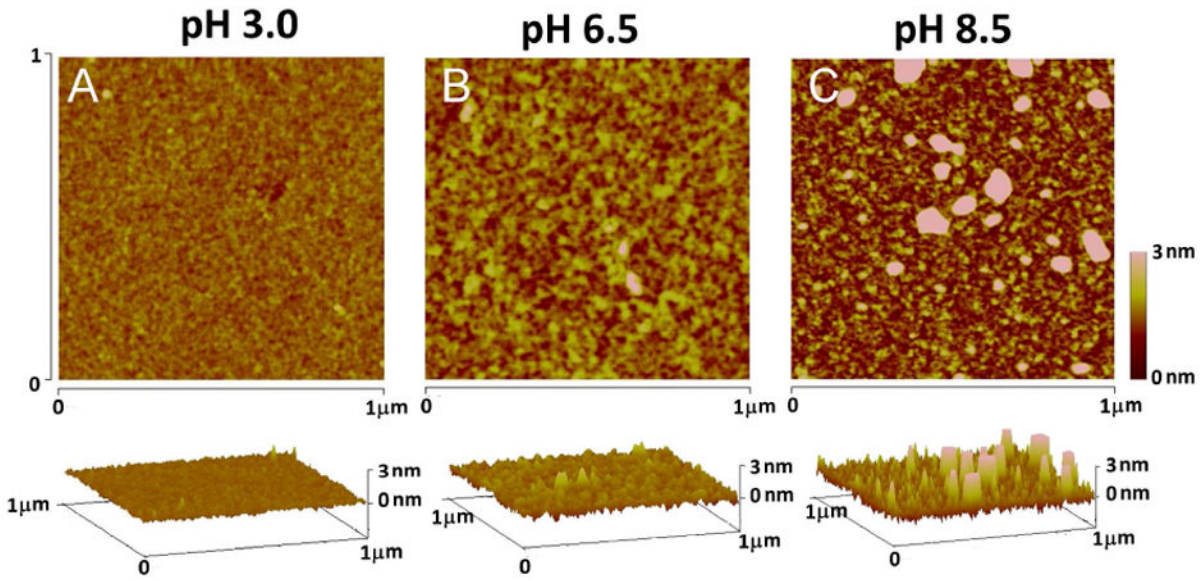

Figure 3.
AFM tapping mode images of chitosan films on freshly cleaved mica deposited at pH3.0 and incubated for 1hr (A) at pH 3.0, (B) at pH 6.5, and (C) at pH 8.5.

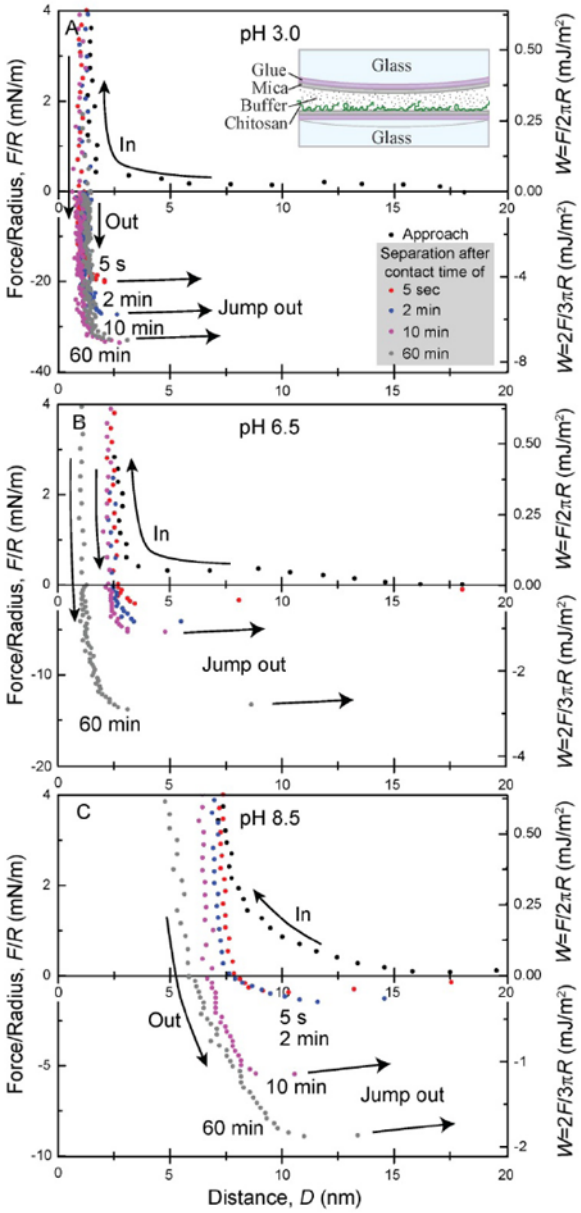

Figure 4.

Force profiles between physisorbed chitosan surfaces against mica in (A) pH 3.0 and 150 mM acetic acid solution, (B) pH 6.5 and 150 mM sodium acetate buffer solution, and (C) pH 8.5 and 150 mM phosphate buffer solution with the contact times of 5 sec, 2 min, 10 min, and 1 hr. All force curves are the representative results at each experiment conditions.

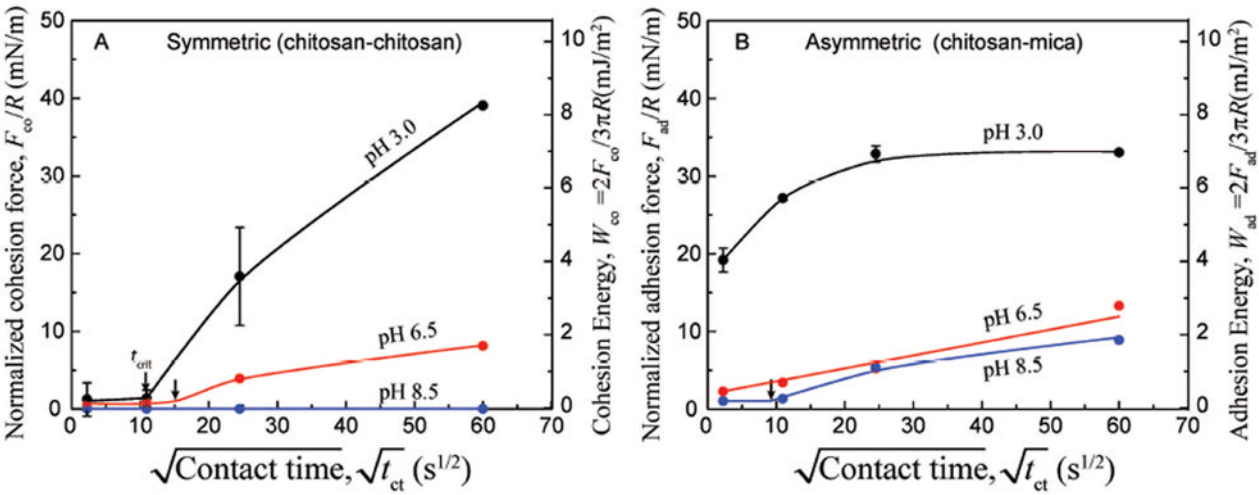

Figure 5.

Normalized cohesion/adhesion force (Energy) *vs* contact time curve for symmetric (chitosan *vs* chitosan) and asymmetric (chitosan *vs* mica) cases under the applied load of ~4 mN/m at pHs of 3.0 (black), 6.5 (red) and 8.5 (blue). Arrows indicate critical contact time, t_{crit}, where surfaces become adhesive.

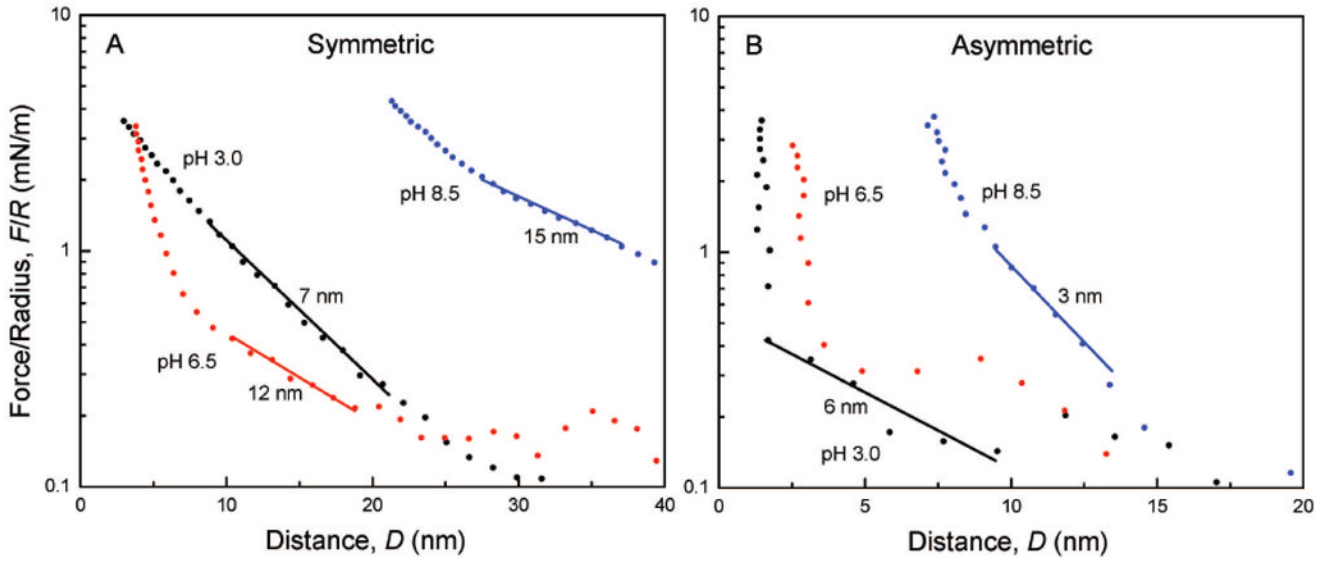

Figure 6.

Approach curves for symmetric and asymmetric cases at pHs of 3.0, 6.5, and 8.5. The calculated Debye lengths were ~2.5, ~0.8, and ~0.8 nm, respectively. The larger decay lengths compared to the Debye lengths indicate that steric contribution is significant on approach for all cases.

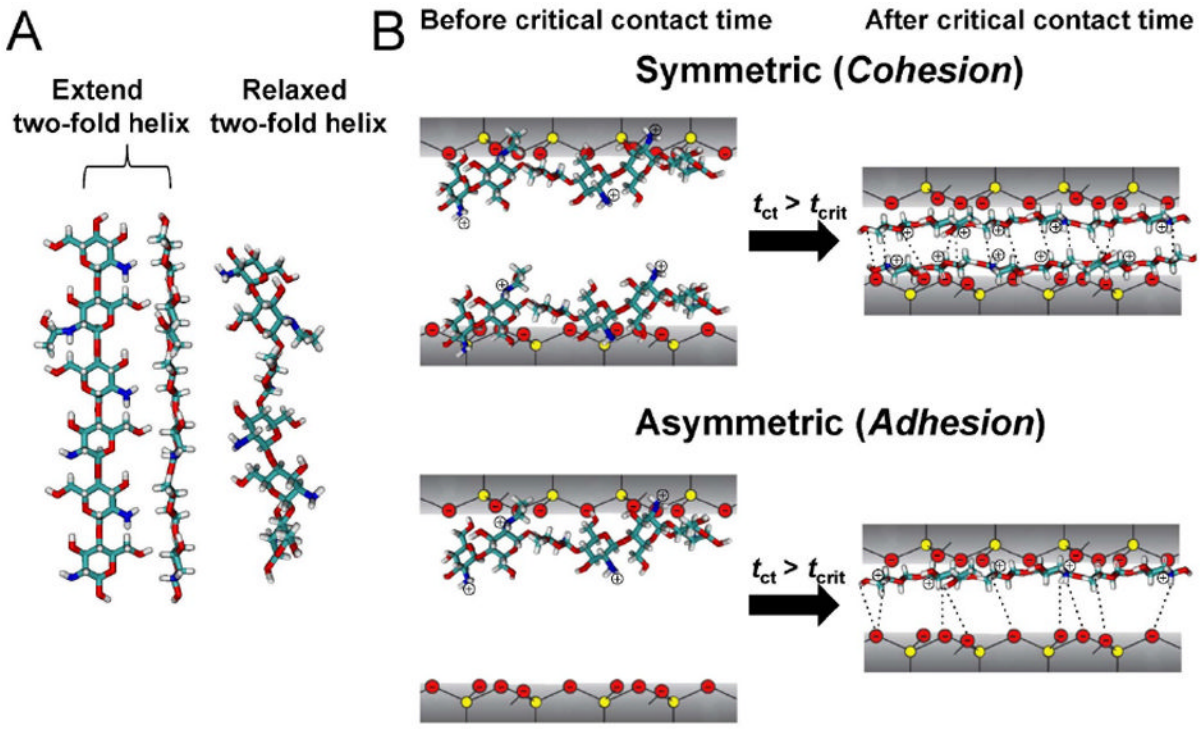

Figure 7.

(A) Molecular structure of chitosan (*left and center*) extended two fold helix[17] and (*right*) relaxed two-fold helix[13] as determined by X-ray crystallography (B) Schematic representation of the putative cohesion (*top right*, chitosan *vs* chitosan) and adhesion (*bottom right*, chitosan *vs* mica) mechanisms of chitosan film in wet conditions. Atoms color coded as: cyan:carbon; red:oxygen; blue:nitrogeon; white:hydrogen; yellow:silicon. Putative hydrogen bonds are shown as dotted lines.